Journal of Magnetic Resonance **147,** 68–77 (2000)
doi:10.1006/jmre.2000.2161, available online at http://www.idealibrary.com on IDEAL®

MAS Double-Quantum Filtered Dipolar Shift Correlation Spectroscopy

Axel S. D. Heindrichs,* Helen Geen,* and Jeremy J. Titman†

*School of Physics and Astronomy and †School of Chemistry, University of Nottingham, University Park, Nottingham NG7 2RD, United Kingdom

Received December 27, 1999; revised June 23, 2000

A carbon-13 magic angle spinning double-quantum filtered dipolar shift correlation NMR experiment which can be used to establish through-space connectivities in solids is analyzed. The main advantage of the double-quantum filtered approach is the removal of intensity arising from natural abundance background signals. The variation in intensity of the cross and diagonal peaks observed in the two-dimensional spectrum as a function of mixing time is investigated experimentally for model systems. The observed behavior is compared with analytical expressions derived for three coupled spins, as well as with simulations based on average Hamiltonian theory.

INTRODUCTION

The double-quantum filtered correlation spectroscopy (DQF-COSY) technique (*1*) is perhaps the most useful of the many two-dimensional solution-state nuclear magnetic resonance (NMR) experiments (*2*) proposed to date. The experiment results in cross peaks in the frequency plane at coordinates determined by the chemical shifts of pairs of through-bond scalar-coupled nuclei. The information about through-bond connectivities obtained from these correlations has proved useful for the structure elucidation of organic molecules from natural products to proteins, as well as inorganic materials. The main advantage over earlier variants of the COSY experiment is the spectral simplification achieved by filtering the observed signal through double-quantum coherence (*3*) corresponding to a normally forbidden transition. In particular, peaks resulting from nuclei with no coupling partners are completely removed from the two-dimensional spectrum.

In solid-state NMR the straightforward combination of DQF-COSY and related experiments with magic angle spinning (MAS) has already proved useful for structural studies of zeolites (*4*). MAS is required in order to remove the spectral broadening due to the anisotropy of nuclear spin interactions such as chemical shifts and dipolar couplings. In favorable cases and with dilute nuclei, such as carbon-13 or silicon-29, the resolution obtained with MAS is sufficiently high to allow the successful operation of the COSY experiment. Recently, progress (*5*) has been made with related experiments by the incorporation of efficient heteronuclear decoupling schemes (*6*) and other procedures to reduce the effective carbon-13 linewidth. In solids, through-space dipolar couplings between spins are generally several orders of magnitude larger than their scalar counterparts and, in contrast to the solution case, are not averaged to zero by rapid isotropic tumbling. Hence, solid-state shift correlation spectroscopy experiments based on magnetization transfer between dipolar-coupled spins are also possible.

The combination of correlation spectroscopy and MAS is not straightforward in the dipolar case, due to the averaging of the dipolar interaction by the spinning (*7*). However, the past few years have seen the advent of "recoupling" sequences (*8, 9*) designed to reintroduce MAS-averaged dipolar couplings between spin-1/2 nuclei. This advance has prompted the development of several solid-state shift correlation experiments based on magnetization transfer mediated by a recoupled dipolar Hamiltonian which operates during the mixing time (*9, 10*). These experiments result in cross peaks at coordinates determined by the chemical shifts of pairs of dipolar-coupled nuclei. This paper concerns a carbon-13 dipolar shift correlation experiment in which the observed signal is filtered through double-quantum coherence after the fashion of DQF-COSY. The main advantage of the DQF approach is the removal of intensity on the diagonal arising from natural abundance background signals, from nuclei with no coupling partners, or from orientations for which dipolar couplings are only weakly reintroduced by the recoupling sequence. A theoretical and experimental comparison of the carbon-13 DQF dipolar shift correlation and the straightforward magnetization transfer approach (*10*) is presented here. The experimental variation in intensity of the cross and diagonal peaks as a function of mixing time is investigated for two model systems: the uniformly carbon-13 labeled amino acids alanine and tyrosine. The observed behavior is compared with analytical expressions derived for three coupled spins, as well as with simulations based on average Hamiltonian theory. A brief demonstration of a related phosphorus-31 experiment (*11*) and a carbon-13 application in which there is a natural abundance background (*12*) to remove have been presented in previous publications.

EXPERIMENTAL

The pulse sequences used to record dipolar correlation spectra in this work are shown in Fig. 1, along with the coherence

1090-7807/00 $35.00

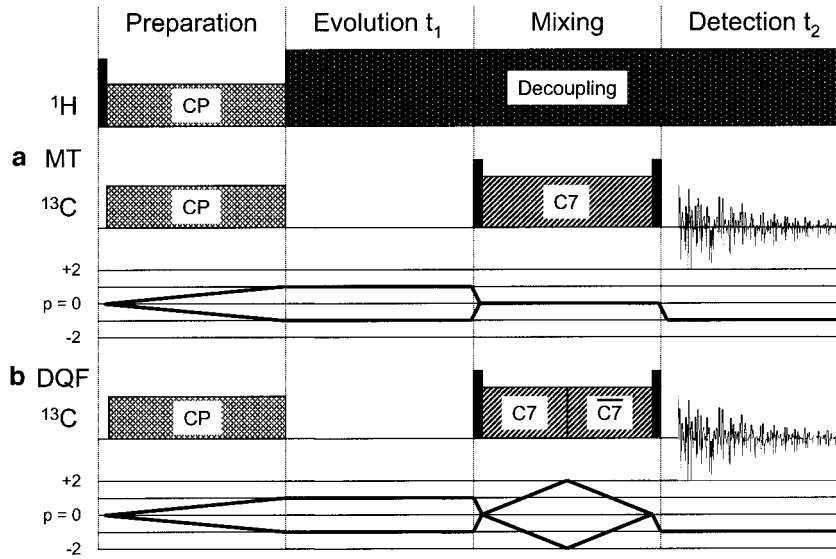

FIG. 1. Pulse sequences and coherence transfer pathways used to record dipolar correlation spectra in this work. During the mixing period magnetization transfer occurs under a recoupled double-quantum dipolar Hamiltonian, generated using the POST-C7 sequence. In the straightforward magnetization transfer experiments (a) there is no time reversal step and the phase cycle simply selects longitudinal magnetization and zero-quantum coherence at the end of the mixing period. For the double-quantum filtered experiment (b) the POST-C7 segments in the first half of the mixing period are phase cycled in order to select double-quantum coherence, as indicated in the coherence transfer pathway. Those occurring during the second half of the mixing period are not cycled but have a constant phase shift of $\pi/2$ to give a time-reversed double-quantum dipolar Hamiltonian.

transfer pathways (*13*). During the preparation period carbon-13 magnetization is generated by cross polarization from neighboring protons. Reproducibility can be improved here by a slight ramp of the carbon-13 field (*14*). At the end of the evolution period t_1 a component of the carbon-13 coherence is transferred to longitudinal magnetization along the z-axis. During the subsequent mixing period magnetization transfer occurs under a recoupled double-quantum dipolar Hamiltonian, generated in this work using the POST-C7 sequence (*15*) due to Hohwy *et al.* POST-C7 contains seven cyclic pulse segments (denoted C) timed to occupy two rotor periods in total, with neighboring C segments differing in their overall phase by $2\pi/7$. For the DQF experiment the POST-C7 segments in the first half of the mixing period are phase cycled in order to select double-quantum coherence, as indicated in the coherence transfer pathway. Those occurring during the second half of the mixing period are not cycled but have a constant phase shift of $\pi/2$ to give a time-reversed double-quantum dipolar Hamiltonian, required for the regeneration of longitudinal magnetization. For mixing times corresponding to nonintegral numbers of POST-C7 cycles, care must be taken with the relative phases of C segments in the first and second halves of the mixing period. In the straightforward magnetization transfer experiments recorded for comparison purposes there is no time reversal step and the phase cycle simply selects longitudinal magnetization and zero-quantum coherence at the end of the mixing period. In both experiments proton decoupling is applied throughout the evolution, mixing, and detection periods. Improved resolution can be obtained in the evolution and detection dimensions with the TPPM decoupling scheme (*16*) due to Bennett *et al.*, although this was not used for the experiments shown here.

Correct operation of the recoupling sequence applied during the mixing period is crucial to maximizing the sensitivity and performance of both straightforward magnetization transfer and DQF dipolar correlation spectra, especially for multispin systems. The main requirements are that the recoupling sequence is insensitive to resonance offset and chemical shift anisotropy, robust with respect to errors such as radiofrequency field inhomogeneity, and efficient in terms of the fraction of the magnetization which survives the double-quantum filter. While magnetization transfer can be achieved with sequences which recouple a zero-quantum dipolar Hamiltonian, this approach is inappropriate for the DQF experiments described here. Hence, for this work we have chosen the POST-C7 sequence (*15*) which generates double-quantum coherence efficiently in a powder because of the simple way in which the recoupled dipolar interaction depends on the orientation of the molecule with respect to the MAS rotor. This property of the parent sevenfold sequence (*17*) has been used recently to excite very high orders of proton multiple-quantum coherence at fast MAS rates (*18*). A further advantage of POST-C7 is the fact that the sevenfold phase shift combined with the properties of the individual C segments removes errors due to resonance offset and offset/inhomogeneity cross terms to high order (*15*). The robust character of POST-C7 makes the broadband recoupling required for dipolar correlations in multispin systems feasible using commercially available instrumentation. More recently

two new recoupling sequences have been proposed which are also particularly suitable for dipolar correlation experiments in multispin systems (*10, 19*).

The zeroth-order effective dipolar Hamiltonian for the POST-C7 recoupling sequence for a pair of spin-1/2 nuclei has been shown (*15*) to be

$$\bar{H}^{(0)}_{C7} = \frac{1}{2}\,\omega_{C7} I_1^+ I_2^+ + \frac{1}{2}\,\omega^*_{C7} I_1^- I_2^-, \qquad [1]$$

with

$$\omega_{C7} = \frac{-343(i + e^{i\pi/14})}{520\pi\sqrt{2}}\,\chi \sin 2\beta \exp(-i\gamma), \qquad [2]$$

where β and γ are two of the Euler angles which relate the molecular frame to the rotor frame and χ is the dipolar coupling constant which depends on internuclear distance r,

$$\chi = -\left(\frac{\mu_0}{4\pi}\right)\frac{\gamma^2\hbar}{r^3}. \qquad [3]$$

In the limit of fast MAS where the spinning rate and the radiofrequency field strength are greater than the range of resonance offsets and the chemical shift anisotropy, this effective double-quantum dipolar Hamiltonian is valid for the multispin systems characteristic of the uniformly labeled samples studied here. The origin of the high efficiency of double-quantum generation with POST-C7 is the γ dependence of the phase as opposed to the amplitude of the recoupled Hamiltonian.

Experiments were recorded with a Varian Chemagnetics Infinity spectrometer operating at a carbon-13 Larmor frequency of 75.46 MHz using the sequence shown in Fig. 1 and a standard 3.2-mm Varian Chemagnetics double-resonance MAS probe. The MAS rate of 13 kHz was stabilized to within 0.1%. Up to 10 cycles of the POST-C7 sequence were used during the mixing time with the carbon-13 radiofrequency field set to 91 kHz. Fine adjustments to the radiofrequency field strength were made by maximizing the efficiency of double-quantum filtration in a one-dimensional experiment. No attempt was made to optimize experimental performance by, for example, restricting the sample to the center portion of the rotor to minimize radiofrequency field inhomogeneity. Proton decoupling during the C7 sequence used a radiofrequency field strength of 150 kHz (limited by hardware considerations), and this level was maintained during the evolution and detection periods. The relaxation delay was 1 or 5 s for alanine and tyrosine, respectively, and the contact time for cross polarization was 1 ms. For the evolution dimension, 64 increments were recorded with a maximum t_1 time of 4.92 ms, while the acquisition time in the detection dimension t_2 was 78.78 ms. The dwell time in both dimensions was set equal to the rotor period at 76.92 μs. The hypercomplex method of States *et al.* (*20*) was used to obtain pure absorption lineshapes in the two-dimensional spectrum. Uniformly labeled U-^{13}C amino acids were purchased from Isotec Inc. and used without further treatment.

THEORY AND SIMULATIONS

In both magnetization transfer and DQF dipolar correlation experiments the informative cross peaks arise from the evolution of the spin system under the recoupled double-quantum dipolar Hamiltonian operating during the mixing period. For simplicity in the following analysis an ideal multispin real double-quantum Hamiltonian of the form

$$H^{DQ} = \sum_{j<k} \frac{\omega_{jk}}{2}\,(I_j^+ I_k^+ + I_j^- I_k^-) \qquad [4]$$

is assumed, where ω_{jk} is a function of both the magnitude and the orientation of the dipolar interaction recoupled between spins j and k. In practice both the form of ω_{jk} and the validity of Eq. [4] as an approximation to the effective Hamiltonian are determined by the nature of the recoupling sequence used. However, it should be noted that the γ-dependent phase of the POST-C7 Hamiltonian which appears in Eq. [1] has no effect on the peak intensities. For a dipolar-coupled spin pair with $\omega_{12} = \omega_D$ the sum magnetization evolves under H^{DQ} as

$$(I_{1z} + I_{2z}) \xrightarrow{H^{DQ}\tau} (I_{1z} + I_{2z})\cos(\omega_D\tau) + i(I_1^+ I_2^+ - I_1^- I_2^-)\sin(\omega_D\tau), \qquad [5]$$

while the difference magnetization is invariant (*21*). The effect of the oscillatory behavior of the sum is a net redistribution of magnetization among the coupling partners, leading to dipolar correlation cross peaks in the two-dimensional spectrum. Equation [5] highlights the fact that magnetization transfer is accompanied by the simultaneous creation of double-quantum coherence, and it is this aspect of the evolution which is central to the double-quantum filtered experiment described here. For the magnetization transfer experiment H^{DQ} operates in an uninterrupted fashion for the whole mixing time of length τ, while for the DQF experiment phase cycling during the first half of the mixing period removes all but the second term of Eq. [5] at time $\tau/2$. This is reconverted to observable magnetization by the time-reversed double-quantum dipolar Hamiltonian which operates for the second half.

For uniformly labeled samples the simple two-spin treatment does not suffice to describe all the spectral features. In multi-

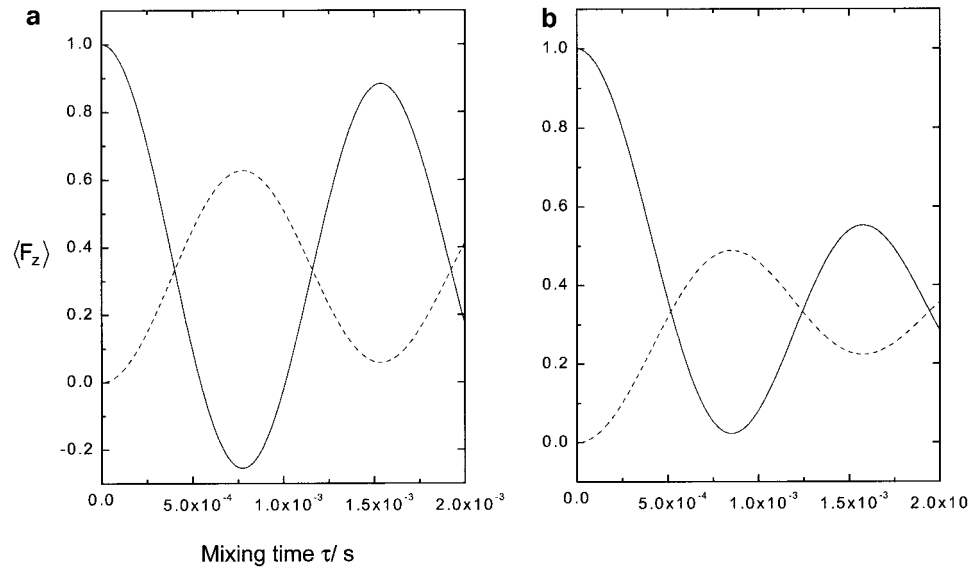

FIG. 2. Simulations of the expectation value of the sum magnetization $\langle F_z \rangle$ as a function of mixing time τ for (full lines) magnetization transfer and (dotted lines) DQF experiments using the POST-C7 average Hamiltonian of Eq. [1]. These are calculated for powder ensembles of spin systems with the limiting (a) triangular and (b) linear topologies described above, except that the internuclear distances used are not exactly equal, but correspond to $\chi_{12} = 2206.5$ Hz and $\chi_{23} = 2080.0$ Hz, with $\chi_{13} = 2142.0$ Hz in (a) and $\chi_{13} = 267.7$ Hz in (b). All of the curves have been normalized so that $\langle F_z \rangle = 1$ for the magnetization transfer experiment at $\tau = 0$.

spin systems there is no simple invariant "difference" magnetization and a general analogue of Eq. [5] is cumbersome. Hohwy *et al.* have defined "magnetization transfer functions" (*19*) for the peak intensities in the straightforward magnetization transfer experiment,

$$S_{jk}^{\mathrm{MT}}(\tau) = \mathrm{Tr}[\exp(-iH^{\mathrm{DQ}}\tau)I_{jz}\exp(iH^{\mathrm{DQ}}\tau)I_{kz}], \qquad [6]$$

where $S_{jk}^{\mathrm{MT}}(\tau)$ is the intensity of the peak at coordinates $(\omega_1, \omega_2) = (\omega_j, \omega_k)$. The analogous function for the DQF experiment is

$$\begin{aligned} S_{jk}^{\mathrm{DQ}}(\tau) = \mathrm{Tr}[&\exp(iH^{\mathrm{DQ}}\tau/2)\hat{P}^{\mathrm{DQ}} \\ &\times \{\exp(-iH^{\mathrm{DQ}}\tau/2)I_{jz}\exp(iH^{\mathrm{DQ}}\tau/2)\} \\ &\times \exp(-iH^{\mathrm{DQ}}\tau/2)I_{kz}], \end{aligned} \qquad [7]$$

where τ is the total mixing time and $\hat{P}^{\mathrm{DQ}}$ is a projection superoperator which retains coherence associated with all the double-quantum transitions at $\tau/2$ as required by the phase cycle. For systems of up to three spins $\hat{P}^{\mathrm{DQ}}$ takes the form

$$\hat{P}^{\mathrm{DQ}} = \sum_{j<k} (|I_j^+ I_k^+\rangle\langle I_j^+ I_k^+| + |I_j^- I_k^-\rangle\langle I_j^- I_k^-|). \qquad [8]$$

For systems of more than three spins, double-quantum terms involving four or more spins must also be taken into account. For a three-spin system Eq. [7] leads to

$$S_{11}^{\mathrm{DQ}}(\tau) = \frac{1}{2}\left\{1 - \frac{1}{\Omega^2}\left[\omega_{23}^2 + (\omega_{12}^2 + \omega_{13}^2)\cos\left(\frac{\sqrt{\Omega}\tau}{2}\right)\right]^2\right\}$$

$$\begin{aligned} S_{12}^{\mathrm{DQ}}(\tau) = \frac{1}{\Omega^2}\Bigg[&\omega_{12}^4 - \omega_{23}^2\omega_{13}^2 + \omega_{12}^2(\omega_{23}^2 + \omega_{13}^2) \\ &+ (\omega_{12}^2 + \omega_{23}^2)(\omega_{12}^2 + \omega_{13}^2)\cos\left(\frac{\sqrt{\Omega}\tau}{2}\right)\Bigg] \\ &\times \sin^2\left(\frac{\sqrt{\Omega}\tau}{4}\right) \end{aligned}$$

$$\begin{aligned} S_{13}^{\mathrm{DQ}}(\tau) = \frac{1}{\Omega^2}\Bigg[&\omega_{13}^4 - \omega_{23}^2\omega_{12}^2 + \omega_{13}^2(\omega_{23}^2 + \omega_{12}^2) \\ &+ (\omega_{13}^2 + \omega_{23}^2)(\omega_{13}^2 + \omega_{12}^2)\cos\left(\frac{\sqrt{\Omega}\tau}{2}\right)\Bigg] \\ &\times \sin^2\left(\frac{\sqrt{\Omega}\tau}{4}\right), \end{aligned} \qquad [9]$$

where $\Omega^2 = \omega_{12}^2 + \omega_{23}^2 + \omega_{13}^2$. As described above, ω_{jk} is an orientation-dependent dipolar interaction and this must be taken into account when using this expression to model powdered samples. In conjunction with the corresponding expression for straightforward magnetization transfer (*19*), Eq. [9] allows the mixing time variation of the peak intensities in the two experiments to be compared. Quantitatively, this comparison reveals a relationship between observed intensities for the

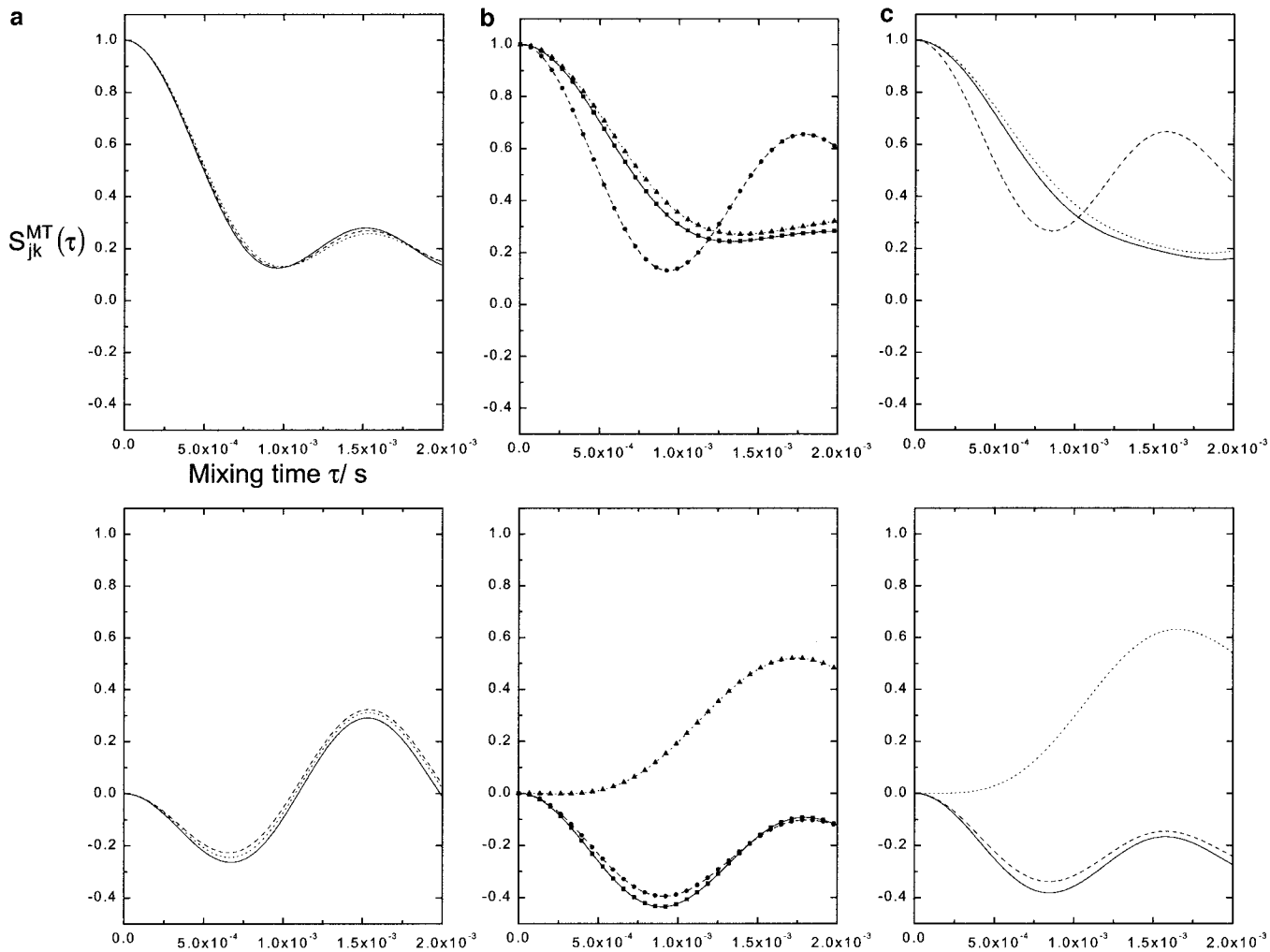

FIG. 3. Simulations of (top) diagonal and (bottom) cross-peak intensities $S_{jk}^{\mathrm{MT}}(\tau)$ for the magnetization transfer experiment as a function of mixing time τ. The spin system mimics that of the three carbon-13 sites in U-^{13}C alanine, except that the CO–α–β bond angle is allowed to vary as follows: (a) 60° (b) 111°, and (c) 180°. For each topology the plots show the three diagonal peaks (CO, solid lines; α-carbon, dashed lines; β-carbon, dotted lines) and three cross peaks (CO–α, solid; α–β, dashed; CO–β, dotted). The latter are averages of pairs of cross peaks related by symmetry about $\omega_1 = \omega_2$. Points in (b) are calculated using the analytical expression of Eq. [9] with $\chi_{13} = 463.5$ Hz. All of the curves have been normalized so that $S_{jk}^{\mathrm{MT}}(\tau) = 1$ experiment at $\tau = 0$.

magnetization transfer and the DQF experiments which for a general three-spin system takes the form

$$S_{jk}^{\mathrm{DQ}}(\tau) = \frac{1}{2}\{1 - S_{jk}^{\mathrm{MT}}(\tau)\} \quad j = k$$

$$S_{jk}^{\mathrm{DQ}}(\tau) = -\frac{1}{2} S_{jk}^{\mathrm{MT}}(\tau) \qquad j \neq k. \qquad [10]$$

Numerical simulations suggest that Eq. [10] is also valid for larger spin systems at short mixing times. The most significant difference is the twofold loss in cross-peak intensity observed for the DQF experiment which must be offset against the advantages of the filter. A further difference is that the cross peaks obtained with the DQF variant are always of opposite sign to their counterparts in the magnetization transfer experiment. Most importantly, however, Eq. [10] demonstrates that, neglecting any spectral simplification due to the double-quantum filter, the information content of the two experiments is identical. All significant features such as maximum cross-peak intensities occur at identical mixing times for the two experiments. The magnetization transfer functions for both experiments are dominated by the strongest couplings. For an equilateral triangle ($\omega_{12} = \omega_{23} = \omega_{13} = \omega_{\mathrm{D}}$) cross-peak functions $S_{12}^{\mathrm{DQ}}(\tau)$ and $S_{13}^{\mathrm{DQ}}(\tau)$ have the same sign and show identical mixing time behavior, whereas for a linear chain ($\omega_{12} = \omega_{23} = \omega_{\mathrm{D}}$ and $\omega_{13} = 0$) the latter is of opposite sign and becomes significant only at longer mixing times. Both the sign inversion and the slow growth of these peaks in linear topologies are characteristic of two-stage "relay" transfer between remote

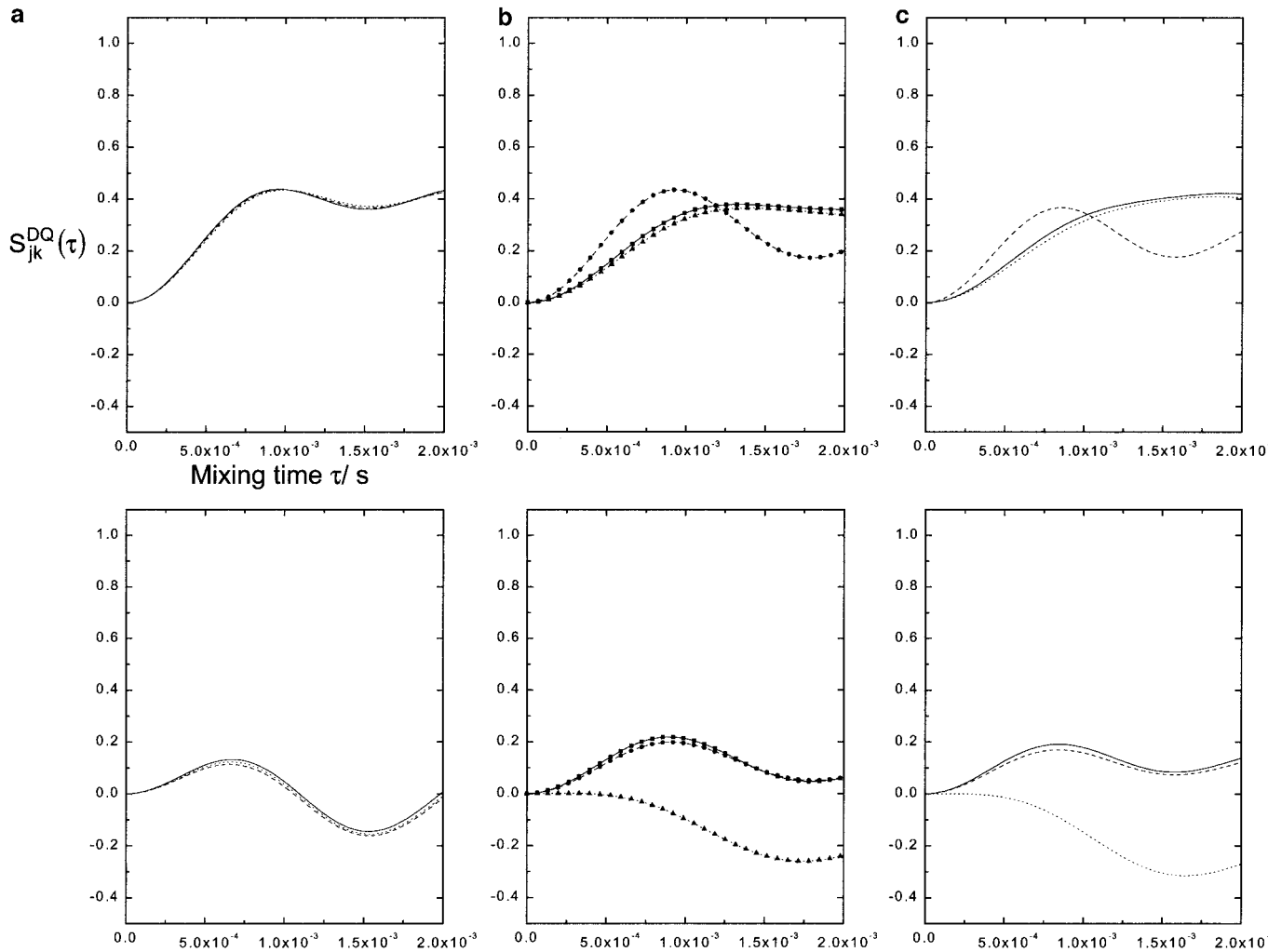

FIG. 4. As in Fig. 3 but for the DQF experiment. The curves have been normalized by the same factors as those in Fig. 3.

spins via a network of direct couplings, a phenomenon which has been observed previously for the magnetization transfer experiments (*10*). The two-stage nature of the remote cross peaks in the DQF experiment is evident from the form of $S_{13}^{DQ}(\tau)$ for which only terms in $\omega_{12}^2\omega_{23}^2$ are nonvanishing for the linear case. Numerical simulations for larger linear spin systems demonstrate that multistage transfer processes occur and the resulting cross peaks alternate in sign for each subsequent relay step. Hence for the DQF variant the direct cross peaks are positive, while two-stage transfer peaks are negative; three-stage relay peaks are expected to be positive once more and so on.

Figure 2 shows the expectation value of the sum magnetization $\langle F_z\rangle = \langle I_{1z} + I_{2z} + I_{3z}\rangle$ as a function of mixing time for (full lines) magnetization transfer and (dotted lines) DQF experiments calculated with the POST-C7 average Hamiltonian of Eq. [1]. The simulations were carried out using the GAMMA (*22*) program and are for powder ensembles of three-spin systems with the (a) triangular and (b) linear topologies described above. However, in order to facilitate comparison with results on U-^{13}C alanine (see below) the internuclear distances used are not exactly equal, but correspond to χ_{12} = 2206.5 Hz and χ_{23} = 2080.0 Hz, with χ_{13} = 2142.0 Hz in (a) and χ_{13} = 267.7 Hz in (b). Comparison of (a) and (b) at short mixing times shows a reduced oscillation frequency in the linear case as expected from Eq. [10] since the small coupling between remote spins 1 and 3 makes a negligible contribution to Ω. This phenomenon is obscured at longer mixing times by the damping which occurs more rapidly for the linear case where the direct couplings are collinear. The maximum sum magnetization for the DQF experiment is a measure of the theoretical recoupling efficiency for POST-C7 and varies from 63 to 50% as a function of topology.

Figures 3 and 4 show average Hamiltonian simulations of $S_{jk}(\tau)$ for (Fig. 3) the magnetization transfer experiment and (Fig. 4) the DQF variant. In each figure both diagonal peak (top) and cross-peak (bottom) intensities are shown for different topologies (a), (b), and (c). The spin system mimics that of

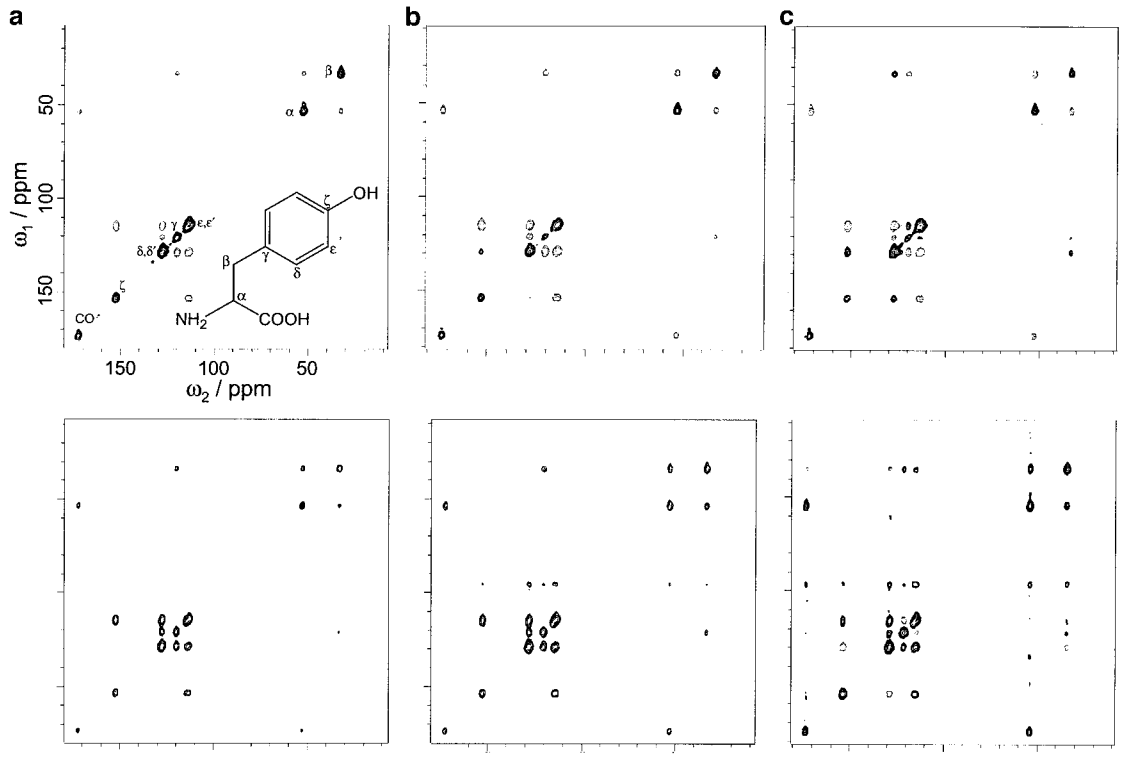

FIG. 5. Two-dimensional magnetization transfer (top) and double-quantum filtered (bottom) correlation spectra on uniformly carbon-13 labeled tyrosine recorded as a function of mixing time with τ set to (a) 308 (b) 615, and (c) 923 μs, respectively. Negative contours are indicated by dotted lines. The peak assignment shown along the diagonal of the magnetization transfer spectrum (a) uses the standard labeling for carbon atoms in amino acid side chains. To aid interpretation, the structure of tyrosine is also shown. The contour levels for each spectrum are chosen so as to reveal as many peaks as possible without significant interference from t_1 noise. At long mixing times peaks at close to zero frequency appear in the DQF spectrum, and similar peaks are present at lower contour levels in the magnetization transfer spectrum.

the three carbon-13 sites in U-^{13}C alanine, except that the CO–α–β bond angle is allowed to vary. The extremes of (a) 60° and (c) 180° compare closely to the simple topologies described above, while (b) (bond angle = 111° χ_{13} = 463.5 Hz) corresponds to the alanine molecule (*23*). The points in Fig. 4b were calculated using Eqs. [6] and [7] with ω_{jk} appropriate for POST-C7 as defined in Eq. [1]. All of the features highlighted by the analytical expressions are confirmed by the simulations. For example, the twofold reduction in intensity and the sign inversion for cross peaks in the DQF experiment (Fig. 4) are clearly demonstrated. Of particular interest is the variation with topology, including the lack of significant discrimination between the linear chain (c) and the alanine molecule (b). For both of these cases the direct CO–α and α–β cross peaks appear at short mixing times, while the relay CO–β peak appears at much longer times. It should be noted that for three-spin systems the relay peak can be the most intense in the spectrum at long times. As expected from Eq. [10] and in contrast to a recent claim (*10*), these peaks are not of low intensity relative to the direct cross peaks in the DQF variant (Fig. 4). For bond angles below 90° there are substantial changes as a function of topology, such that for the triangle (a) all cross peaks show identical mixing time behavior, including an overall sign inversion at long times. Figure 3 also highlights the effect on peak intensities of an orientation-dependent dipolar Hamiltonian in an isotropic powder sample. A part of the magnetization arising from molecules with unfavorable orientations for recoupling remains on the diagonal for the magnetization transfer experiment and is removed completely by the filter in the DQF variant. Similar numerical calculations for larger spin systems have been carried out, and the relationship in Eq. [10] has been confirmed for a range of topologies. Finally we note that the results of the average Hamiltonian simulations described here have been confirmed by exact piecewise calculations based on numerical integration of the propagator over a single POST-C7 cycle.

RESULTS AND DISCUSSION

Figure 5 shows two-dimensional magnetization transfer (top) and DQF (bottom) dipolar correlation spectra on 99% U-^{13}C tyrosine recorded with mixing times ranging from (a) 308 to (c) 923 μs. Negative contours are indicated by dotted lines. As expected from Eq. [10], both direct cross peaks and

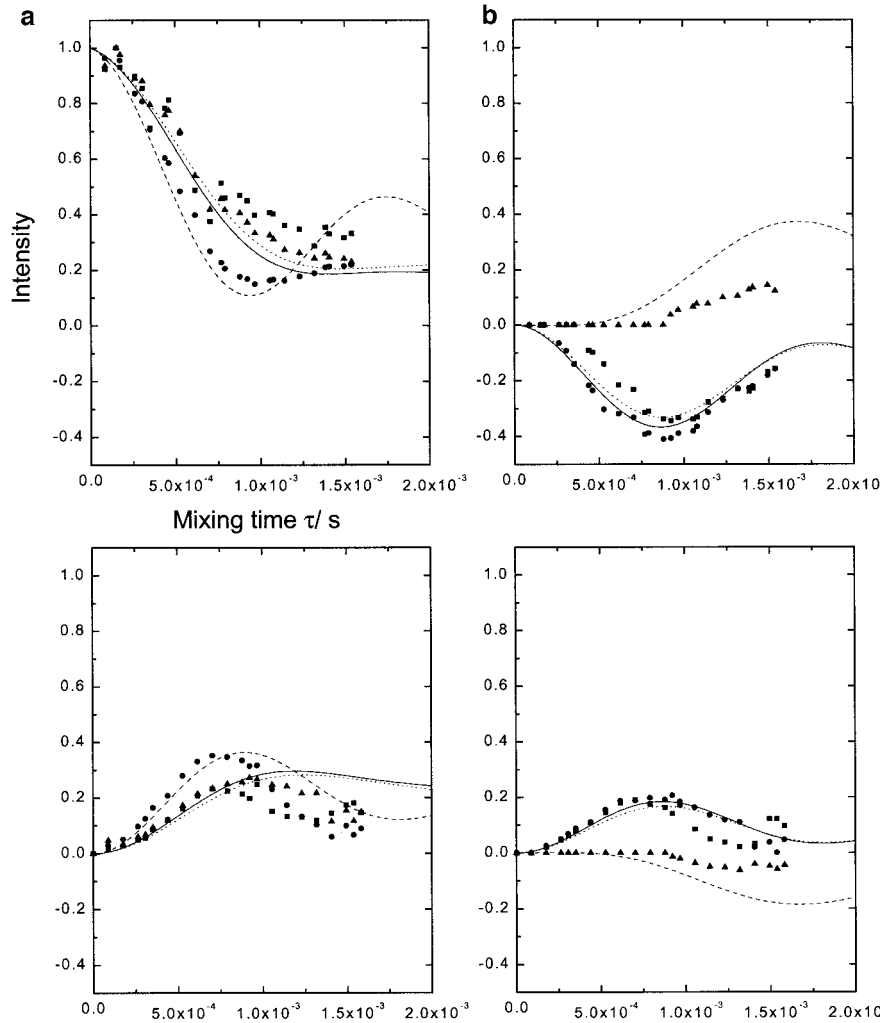

FIG. 6. A comparison between simulated peak intensities of Fig. 3 (lines) and experimental measurements (points) on 99% U-^{13}C alanine as a function of mixing time with (a) showing diagonal and (b) cross peaks for the straightforward (top) and the double-quantum filtered (bottom) experiment, respectively. The cross-peak intensities are averages of pairs of cross peaks related by symmetry about $\omega_1 = \omega_2$. The experimental data were normalized according to the procedure described in the text. The calculated data were damped by an exponential function with a time constant of 5 ms to take account of signal losses during the mixing time.

relay peaks occur at identical frequency coordinates at similar mixing times in the two spectra, suggesting that dipolar correlations between spins can be established with equal veracity using either experiment. At the shortest mixing time all of the expected one bond correlations are present in both spectra, as can easily be verified from the assignment shown on the diagonal peaks (Fig. 5a, top). In the straightforward magnetization transfer spectrum the cross peaks have the opposite sign to and are significantly less intense than the diagonal. On the other hand, as predicted by Eq. [10] in the DQF spectrum, cross and diagonal peaks have the same sign and are of similar magnitude to one another. It should be noted that the diagonal peaks in the magnetization transfer experiment are more intense relative to the cross peaks than expected from the numerical simulations. For the 99% U-^{13}C sample used here this effect cannot be ascribed to natural abundance background signals. The additional contribution arises from deficiencies in the recoupling quality due to experimental imperfections which are not taken into account in the numerical simulations. As with the signal arising from molecules in unfavorable orientations for recoupling, this magnetization is completely removed by the filter in the DQF variant. This contribution to the diagonal is an additional source of t_1 noise in the magnetization transfer experiment which, to some extent, overcomes the sensitivity advantage relative to the DQF variant. At longer mixing times two-stage relay transfer peaks appear in the spectra with opposite sign to the one-bond correlations. Of particular note is the β-carbon which shows two-stage correlations to the CO- and δ-carbons and, in the double-quantum filtered spectrum, a positive three-stage relay peak to the ϵ-car-

bon. As demonstrated above, this sign alternation is expected for the somewhat linear coupling topology encountered in the tyrosine side chain.

Figure 6 shows a comparison between the simulated peak intensities of Figs. 3 and 4 (lines) and experimental measurements (points) on uniformly carbon-13 labeled alanine as a function of mixing time with (a) showing diagonal and (b) cross peaks for the straightforward (top) and the DQF (bottom) experiment, respectively. The experimental recoupling efficiency for POST-C7 was measured by comparing the maximum total intensity in the DQF spectrum with the total intensity for the magnetization transfer experiment at the same mixing time. This procedure results in an efficiency of 38% which should be compared to the 58% calculated theoretically for this topology. This factor was used to scale down the diagonal peak intensities of the magnetization transfer spectrum to account for the contribution which was not recoupled due to experimental imperfections. Finally, peaks in all spectra were normalized to the scaled intensity of the corresponding magnetization transfer diagonal peak at $\tau = 0$. All of the calculated data (taken from Figs. 3b and 4b) was damped by an exponential function with the same time constant of 5 ms to take account of signal losses which arise from incomplete proton decoupling during the POST-C7 sequence and from relaxation (*24*) during the POST-C7 sequence. The main features of the experimental curves, such as maximum cross-peak intensities and the onset of two-stage transfer, are in tolerable agreement with the calculated data. It should be noted that a better match can be achieved by using a different time constant for each group of peaks in the two-dimensional spectrum and that this procedure has been proposed in a recent analysis of double-quantum spectra (*25*).

A final point of interest is the somewhat surprising success of both magnetization transfer and DQF experiments at the relatively high MAS rate of 13 kHz used here. The 150-kHz field strength of the proton decoupling applied during the mixing period is less than twice the 91-kHz carbon-13 field used for the POST-C7 sequence. Previous experimental work (*10*) at low MAS rates has suggested that a mismatch in the two field strengths of a factor of 3 is required during the mixing period in order to prevent depolarization of the carbon-13 spins. However, the data shown in Fig. 6 suggest that this requirement can be relaxed significantly at higher MAS rates and proton decoupling field strengths.

CONCLUSIONS

The double-quantum filtered shift correlation experiment has been shown to be useful for establishing through-bond connectivities, providing identical information about dipolar coupling topologies to the straightforward magnetization experiment. Even with U-^{13}C labeled model amino acid systems the diagonal peak intensities can be reduced by the incorporation of the double-quantum filter which removes signal arising from both experimental imperfections and molecules in unfavorable orientations for recoupling. For real samples with only partial isotopic enrichment, the removal of the natural abundance background by the double-quantum filter proves to be indispensable. The attenuation of the intense diagonal provides spectral simplification and reduces t_1 noise. In principle, analytical expressions such as Eq. [9] and simulations as shown in Figs. 3 and 4 can be used to determine coupling topologies and, therefore, bond lengths and approximate dihedral angles.

ACKNOWLEDGMENTS

This research was supported by the EPSRC (Grant GR/L26742). ASDH thanks the EPSRC for a studentship and HG the Royal Society for a University Research Fellowship. We are grateful to Dr T. de Swiet (Nottingham) for reading the manuscript.

REFERENCES

1. U. Piantini, O. W. Sørensen, and R. R. Ernst, *J. Am. Chem. Soc.* **104,** 6800 (1982).
2. R. R. Ernst, G. Bodenhausen, and A. Wokaun, "Principles of Nuclear Magnetic Resonance in One and Two Dimensions," Oxford Univ. Press, Oxford, 1987.
3. A. Wokaun and R. R. Ernst, *Chem. Phys. Lett.* **52,** 407 (1977).
4. C. A. Fyfe, Y. Feng, H. Grondey, C. T. Kokotailo, and H. Gies, *Chem. Rev.* **91,** 1525 (1991).
5. A. Lesage, C Auger, S. Caldarelli, and L. Emsley, *J. Am Chem. Soc.* **119,** 7867 (1997).
6. A. Bielecki, A. C. Kolbert, and M. H. Levitt, *Chem. Phys. Lett.* **155,** 341 (1989).
7. E. M. Menger, S. Vega, and R. G. Griffin, *J. Am. Chem. Soc.* **108,** 2215 (1986).
8. R. Tycko and G. Dabbagh, *Chem. Phys. Lett.* **173,** 461 (1990); N. C. Nielsen, H. Bildsøe, H. J. Jakobsen, and M. H. Levitt, *J. Chem. Phys.* **101,** 1805 (1994); D. M. Gregory, D. J. Mitchell, J. A. Stringer, S. Kiihne, J. C. Shiels, J. Callahan, M. A. Mehta, and G. P. Drobny, *Chem. Phys. Lett.* **246,** 654 (1995); R. Verel, M. Baldus, M. Ernst, and B. H. Meier, *Chem. Phys. Lett.* **287,** 421 (1998); M. Baldus, D. G. Geurts, and B. H. Meier, *Solid-State NMR* **11,** 157 (1998).
9. A. E. Bennett, J. H. Ok, R. G. Griffin, and S. Vega, *J. Chem. Phys.* **96,** 8624 (1992); B.-Q. Sun, P. R. Costa, D. Kosciko, P. T. Lansbury, and R. G. Griffin, *J. Chem. Phys.* **102,** 702 (1995); M. Baldus and B. H. Meier, *J. Magn. Reson.* **128,** 172 (1997).
10. C. M. Rienstra, M. E. Hatcher, L. J. Mueller, B-Q. Sun, S. W. Fesik, and R. G. Griffin, *J. Am. Chem. Soc.* **120,** 10602 (1998).
11. H. Geen, J. Gottwald, R. Graf, I. Schnell, H. W. Spiess, and J. J. Titman, *J. Magn. Reson.* **125,** 224 (1997).
12. T. M. De Swiet, J. L. Yarger, T. Wagberg, J. Hone, B. Gross, M. Tomaselli, J. J. Titman, A. Zettl, and M. Mehring, *Phys. Rev. Lett.* **84,** 717 (2000).
13. G. Bodenhausen, H. Kogler, and R. R. Ernst, *J. Magn. Reson.* **58,** 370 (1984).
14. G. Metz, X. Wu, and S. O. Smith, *J. Magn. Reson. A* **110,** 219 (1994).
15. M. Hohwy, H. J. Jakobsen, M. Edén, M. H. Levitt, and N. C. Nielsen, *J. Chem. Phys.* **108,** 2686 (1998).
16. A. E. Bennett, C. M. Reinstra, M. Auger, K. V. Lakshmi, and R. G. Griffin, *J. Chem. Phys.* **103,** 6951 (1995).

17. Y. K. Lee, N. D. Kurur, M. Helmle, O. Johannessen, N. C. Nielsen, and M. H. Levitt, *Chem. Phys. Lett.* **242,** 304 (1995).

18. H. Geen, R. Graf, A. S. D. Heindrichs, B. S. Hickman, I. Schnell, H. W. Spiess, and J. J. Titman, *J. Magn. Reson.* **138,** 167 (1999).

19. M. Hohwy, C. M. Rienstra, C. P. Jaroniec, and R. G. Griffin, *J. Chem. Phys.* **110,** 7983 (1999).

20. D. J. States, R. A. Haberkorn, and D. J. Ruben, *J. Magn. Reson.* **48,** 286 (1982).

21. B. H. Meier, *Adv. Magn. Reson.* **18,** 1 (1994).

22. S. A. Smith, T. O. Levante, B. H. Meier, and R. R. Ernst, *J. Magn. Reson. A* **106,** 75 (1994).

23. S. Kiihne, M. A. Mehta, J. A. Stringer, D. M. Gregory, J. C. Shiels, and G. P. Drobny, *J. Chem. Phys. A* **102,** 2274 (1998).

24. X. Feng, P. J. E. Verdegem, Y. K. Lee, D. Sandström, M. Edén, P. Bovee-Geurts, W. J. de Grip, J. Lugtenburg, H. J. M. de Groot, and M. H. Levitt, *J. Am. Chem. Soc.* **119,** 6853 (1997).

25. A. Brinkmann, M. Edén, and M. H. Levitt, *J. Chem. Phys.* **112,** 8539 (2000).